CHAPTER IV

RESULTS AND DISCUSSION

4.1 Effect of Combination of Li–Al–B–H System

Various molar ratios of $LiAlH_4$ and $LiBH_4$ in the mixtures were studied in order to understand the effect of the hydride combination on the amount of desorbed hydrogen and the desorption/absorption temperature. As shown in Figure 4.1, $LiAlH_4$ decomposes into two steps starting at 145°C and continues to 220°C with the total hydrogen amount of 7.6 wt%. $LiBH_4$ starts to decompose at a very low temperature of 75°C. A possible reason for the low desorption temperature might be due to the milling process. A small amount of hydrogen about 0.1–1.0 wt% is released between 95 and 300°C. In the case of the $LiAlH_4$–$LiBH_4$ mixtures, a 2:1 $LiAlH_4$:$LiBH_4$ molar ratio releases the highest amount of hydrogen at 6.6 wt%, and it desorbes hydrogen in the temperature range of 100–220°C, as shown in Table 4.1 and Figure 4.1. However, no absorption was observed for any of the samples.

Table 4.1 Desorption amounts (wt%) and temperatures (°C) of $LiAlH_4$–$LiBH_4$ mixtures

Sample	Desorption Temperature (°C)		Desorption Amount (wt%)
	Initial	Final	
$LiAlH_4$	145	220	7.6
1:1	105	220	5.2
2:1	100	220	6.6
3:1	95	220	6.1
4:1	105	220	5.8
1:2	95	210	3.3
$LiBH_4$	75	370*	1.0*

*The final desorption temperature of LiBH4 (370°C) according to the operating condition of this work.

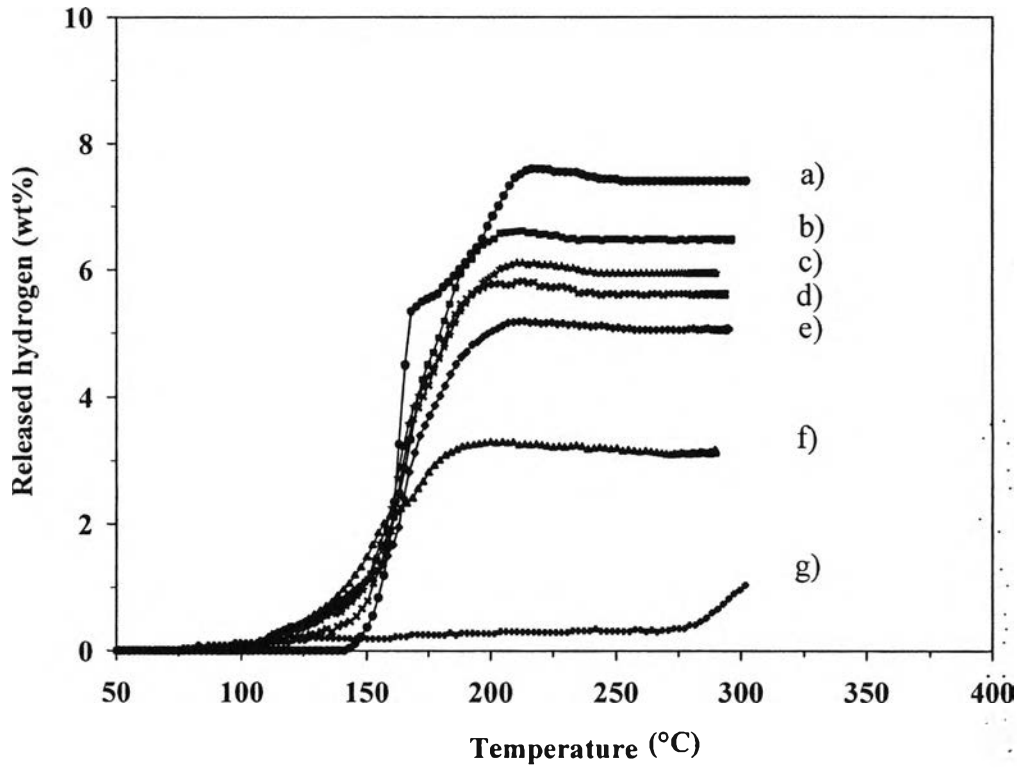

Figure 4.1 Correlation between temperature and hydrogen capacity during the desorption of (a) as-milled $LiAlH_4$; (b) $2LiAlH_4+LiBH_4$; (c) $3LiAlH_4+LiBH_4$; (d) $4LiAlH_4+LiBH_4$ (e) $LiAlH_4+LiBH_4$; (f) $LiAlH_4+2LiBH_4$; and (g) as-milled LiBH4.

4.2 Effect of Catalysts on Hydrogen Desorption in the Li–Al–H Systems

4.2.1 Effect of Catalysts

To study the effect of catalyst types on the hydrogen desorption of $LiAlH_4$, 1 mol% of TiO_2, $TiCl_3$, VCl_3, or $ZrCl_4$ was added to $LiAlH_4$. Blanchard *et al.* (2004) reported that $LiAlD_4$ in the presence of VCl_3 or $TiCl_3 \cdot 1/3(AlCl_3)$ could reduce its thermal decomposition temperature by 60 and 50°C, respectively. The effect of TiO_2 on hydrogen storage properties in $LiAlH_4$-$LiBH_4$ was reported by Mao *et al.* (2009). TiO_2 decreased the temperature of the first and second decomposition steps by 27 and 50°C, respectively. Adding $ZrCl_4$ resulted in the decrease in the first releasing temperature by 40°C and the increase in the desorption kinetics according to Suttisawat *et al.* (2007). Figure 4.2 exhibits the two-step decomposition reactions of both undoped and doped $LiAlH_4$. $LiAlH_4$ starts to decompose around

145°C in the first step and releases about 5.6 wt% hydrogen, while the second step begins to release hydrogen around 180°C and continues to 220°C with 2.0 wt% hydrogen released. The results agree with Blanchard *et al.* (2004), who reported that the first decomposition of $LiAlH_4$ takes place at 150–175°C. While the second step occurs at about 180–220°C.

Moreover, it was clearly observed from Figure 4.2 that all of the additives lower the onset temperature in the first and second steps of the hydrogen desorption, improve the amount of hydrogen released. TiO_2 doped-$LiAlH_4$ provides the highest amount of hydrogen desorption, 8.6 wt%, in the temperature range of 80–195°C. $LiAlH_4$ in the presence of VCl_3 shows the lowest initial temperature of the hydrogen desorption (52°C), which is lower than the undoped one by 93°C, and the amount of hydrogen reaches up to 8.5 wt%. While $LiAlH_4$ in the presence of $ZrCl_4$ shows the lowest final temperature of the hydrogen desorption (155°C), which is lower than the undoped one by 65°C, and the total amount of the hydrogen desorption is 8.1 wt%. The results were summarized in the Table 4.2

Table 4.2 Desorption amount (wt%) and temperature (°C) of doped $LiAlH_4$ in the first (R1) and second (R2) steps

Sample	Desorption Temperature (°C)			Desorption Amount (wt%)		Total wt%
	R1	R2	Final	R1	R2	
As-milled $LiAlH_4$	145	180	220	5.6	2.0	7.6
1 mol% TiO_2–$LiAlH_4$	80	145	195	6.4	2.2	8.6
1 mol% $TiCl_3$–$LiAlH_4$	72	132	185	6.1	2.2	8.3
1 mol% VCl_3–$LiAlH_4$	52	128	180	6.5	2.0	8.5
1 mol% $ZrCl_4$–$LiAlH_4$	80	108	155	5.9	2.2	8.1

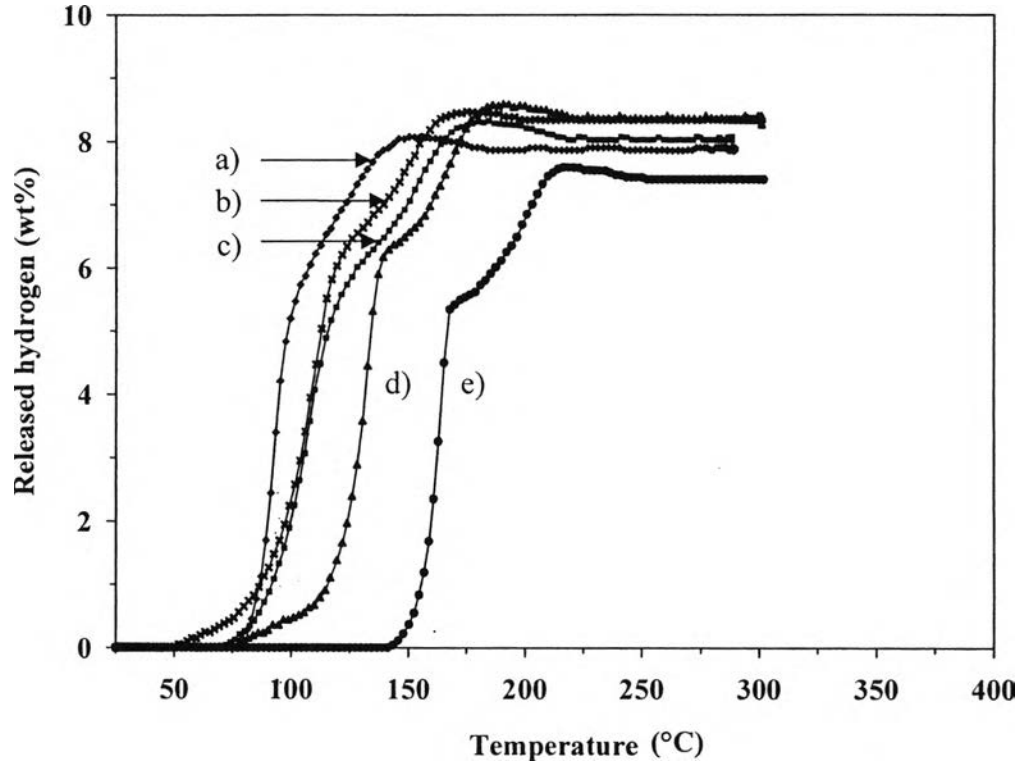

Figure 4.2 Correlation between temperature and hydrogen capacity during the desorption of: (a) 1 mol% $ZrCl_4$–$LiAlH_4$; (b) 1 mol% VCl_3–$LiAlH_4$; (c) 1 mol% $TiCl_3$–$LiAlH_4$ (d) 1 mol% TiO_2–$LiAlH_4$; and (e) as-milled $LiAlH_4$.

4.2.2 Reversibility

No hydrogen absorption was observed for any of the $LiAlH_4$ samples at 120°C and under an 8.5 MPa hydrogen for 12 h. This result agrees with Suttisawat *et al.* (2007), reported that no hydrogen absorption was observed for 4 mol% $ZrCl_4$–$LiAlH_4$ or 4 mol% $HfCl_4$–$LiAlH_4$.

4.3 Effect of Catalysts on Hydrogen Desorption in the Li–B–H Systems

4.3.1 Effect of Catalysts

The effect of catalyst types on the hydrogen desorption of $LiBH_4$ was studied by adding 1 mol% of TiO_2, $TiCl_3$, VCl_3, or $ZrCl_4$ to $LiBH_4$. The desorption was performed from room temperature to 350°C. Züttel *et al.* (2003a) reported that a

small amount of 0.3–1.5 wt% hydrogen was observed between 100 and 200°C for the decomposition of $LiBH_4$. Figure 4.3 shows the first cycle of $LiBH_4$ decomposition. For undoped $LiBH_4$, a small amount of 0.1–1.0 wt% hydrogen is obtained between 95 and 300°C and reaches 3.0 wt% hydrogen at 370°C. Adding 1 mol% catalyst does not show any significant difference in the decomposition temperature or the amount of hydrogen desorption except TiO_2. However, doping with 1 mol% $TiCl_3$ shows the best result that the total amount of 3.5 wt% hydrogen is obtained between 65 and 355°C, while adding 1 mol% TiO_2 results in the decrease in the amount of hydrogen released. Only 2.1 wt% hydrogen is desorbed between 75 and 360°C.

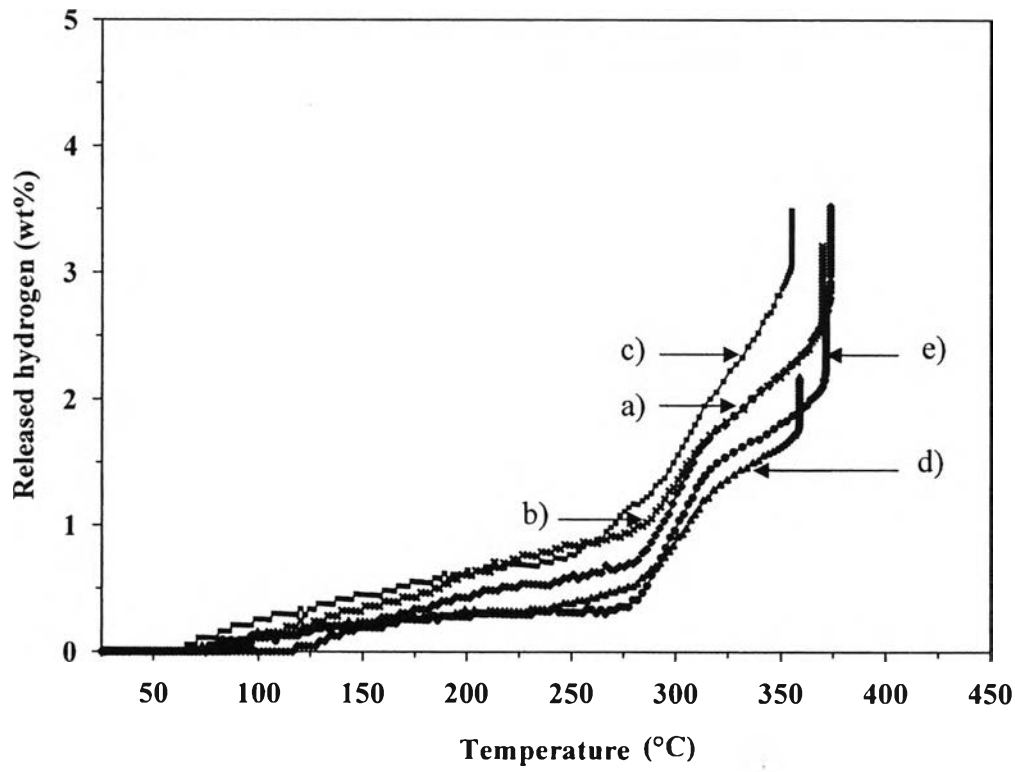

Figure 4.3 Correlation between temperature and hydrogen capacity during the 1st desorption of: (a) 1 mol% $ZrCl_4$–$LiBH_4$; (b) 1 mol% VCl_3–$LiBH_4$; (c) 1 mol% $TiCl_3$–$LiBH_4$; (d) 1 mol% TiO_2–$LiBH_4$; and (e) as-milled $LiBH_4$.

4.3.2 Reversibility

The absorption was done at 300°C and under an 8.5 MPa hydrogen for 6 h. No hydrogen absorption of undoped $LiBH_4$ was observed. On the other hand, doping 1 mol% additives can improve the reversibility of $LiBH_4$ for at least three cycles, as shown in Figures 4.4–4.9.

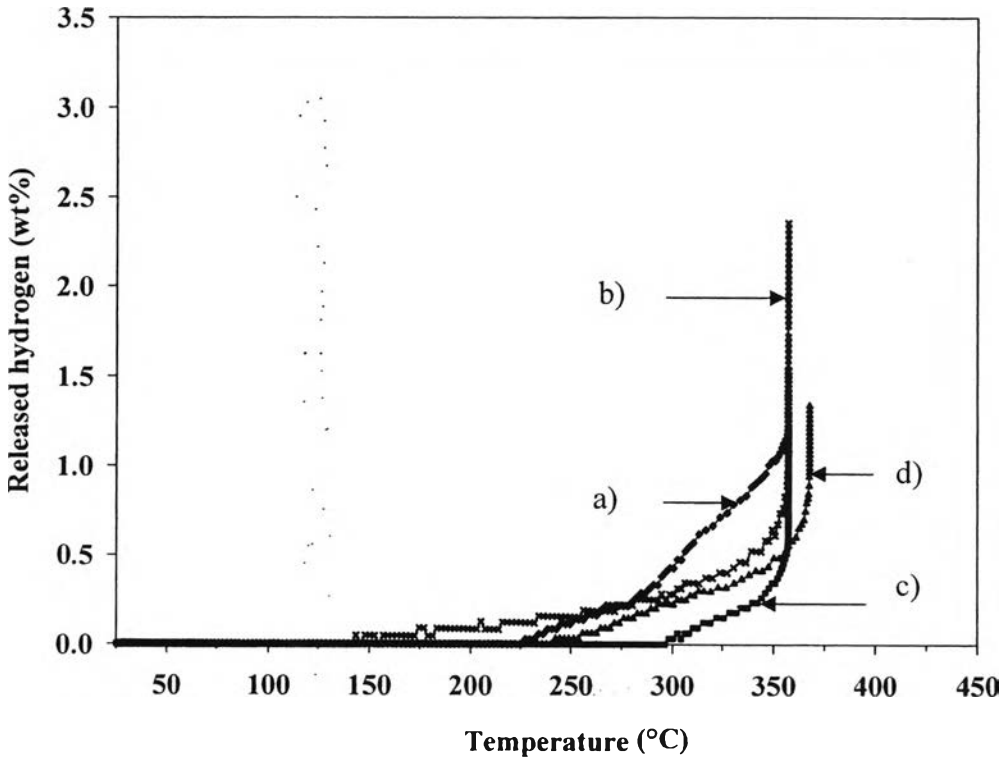

Figure 4.4 Correlation between temperature and hydrogen capacity during the 2nd desorption of: (a) 1 mol% $ZrCl_4$–$LiBH_4$; (b) 1 mol% VCl_3–$LiBH_4$; (c) 1 mol% $TiCl_3$–$LiBH_4$; and (d) 1 mol% TiO_2–$LiBH_4$.

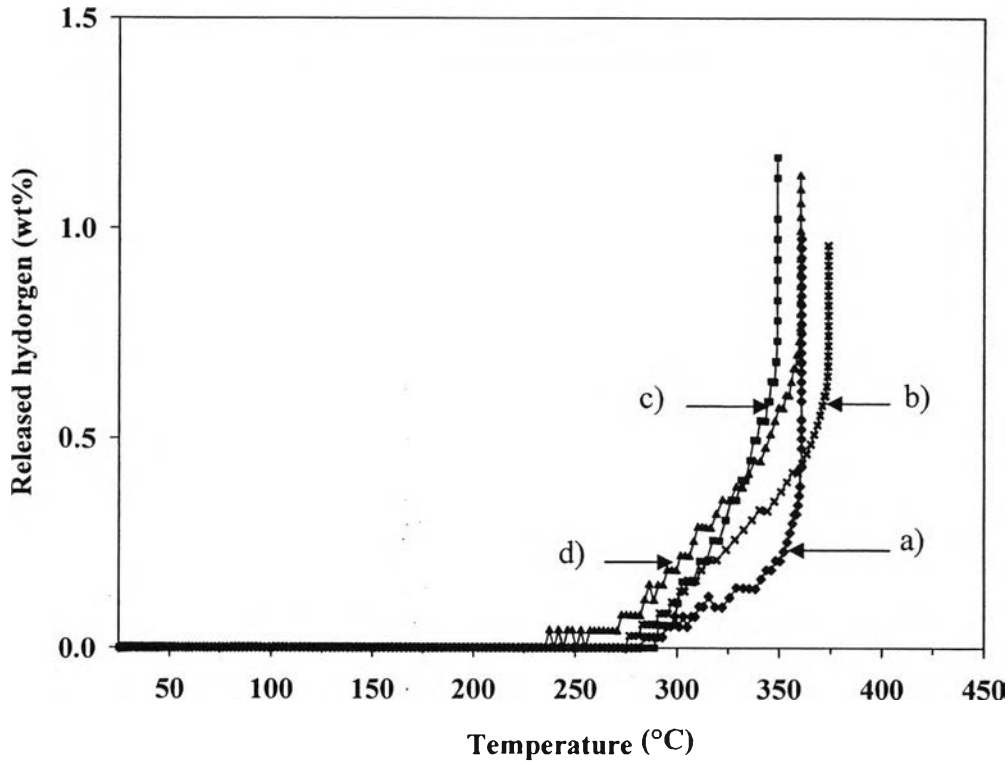

Figure 4.5 Correlation between temperature and hydrogen capacity during the 3rd desorption of: (a) 1 mol% $ZrCl_4$–$LiBH_4$; (b) 1 mol% VCl_3–$LiBH_4$; (c) 1 mol% $TiCl_3$–$LiBH_4$; (d) and 1 mol% TiO_2–$LiBH_4$.

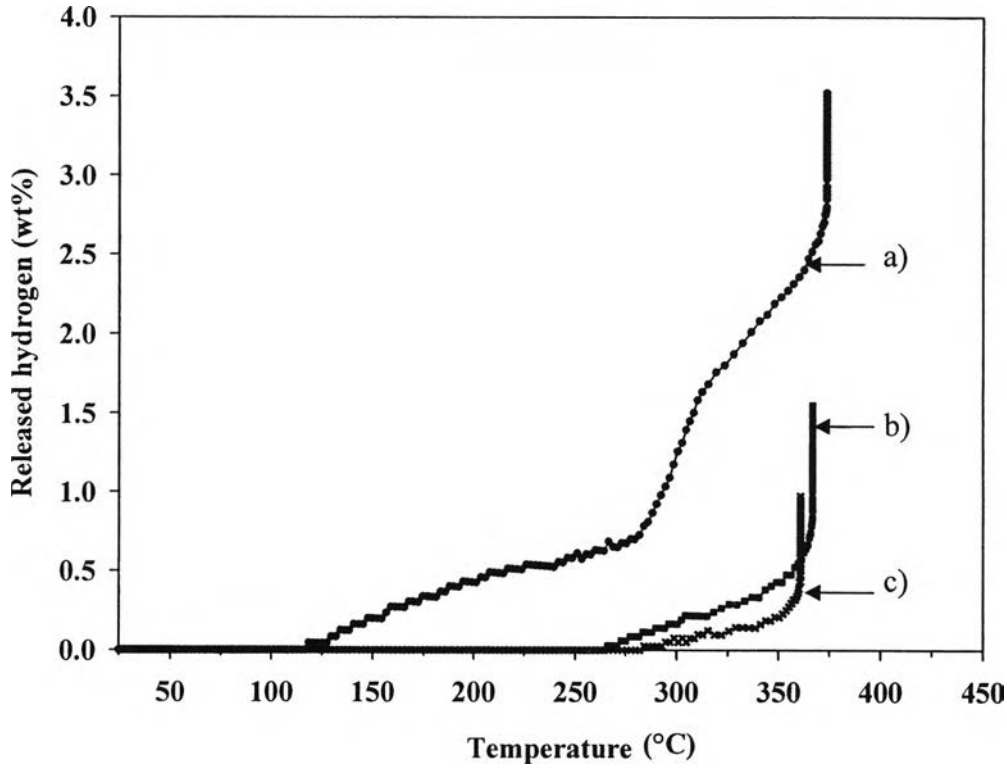

Figure 4.6 Correlation between temperature and hydrogen capacity during the desorption of 1 mol% $ZrCl_4$–$LiBH_4$ in the: (a) 1st desorption; (b) 2nd desorption; and (c) 3rd desorption.

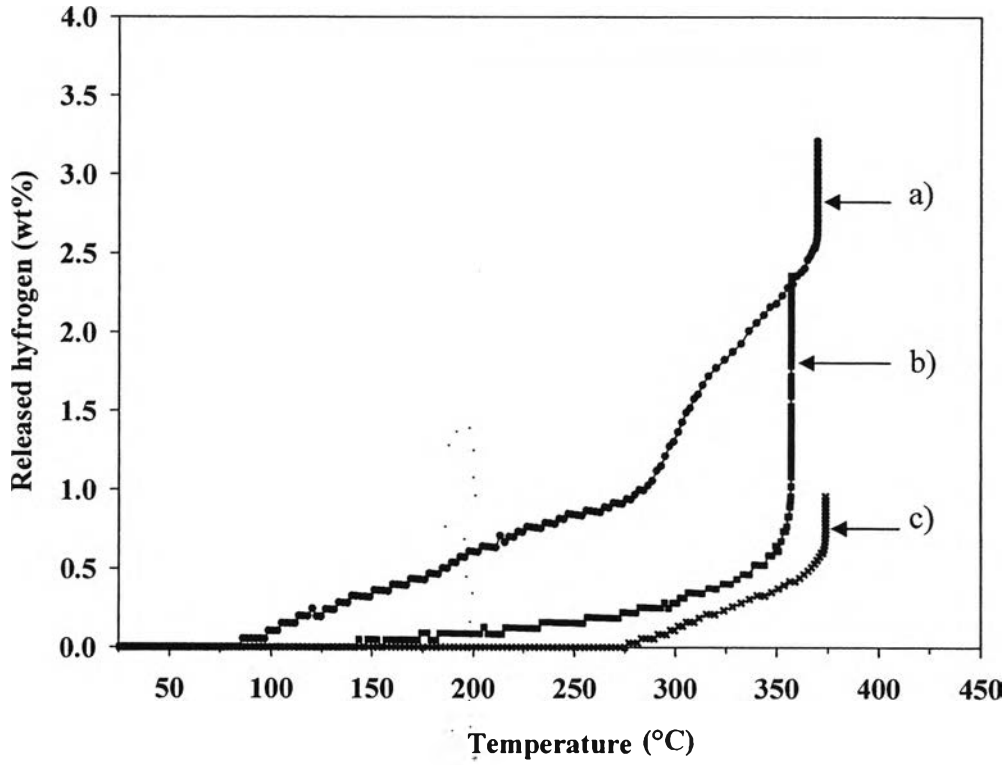

Figure 4.7 Correlation between temperature and hydrogen capacity during the desorption of 1 mol% VCl_3–$LiBH_4$ in the: (a) 1st desorption; (b) 2nd desorption; and (c) 3rd desorption.

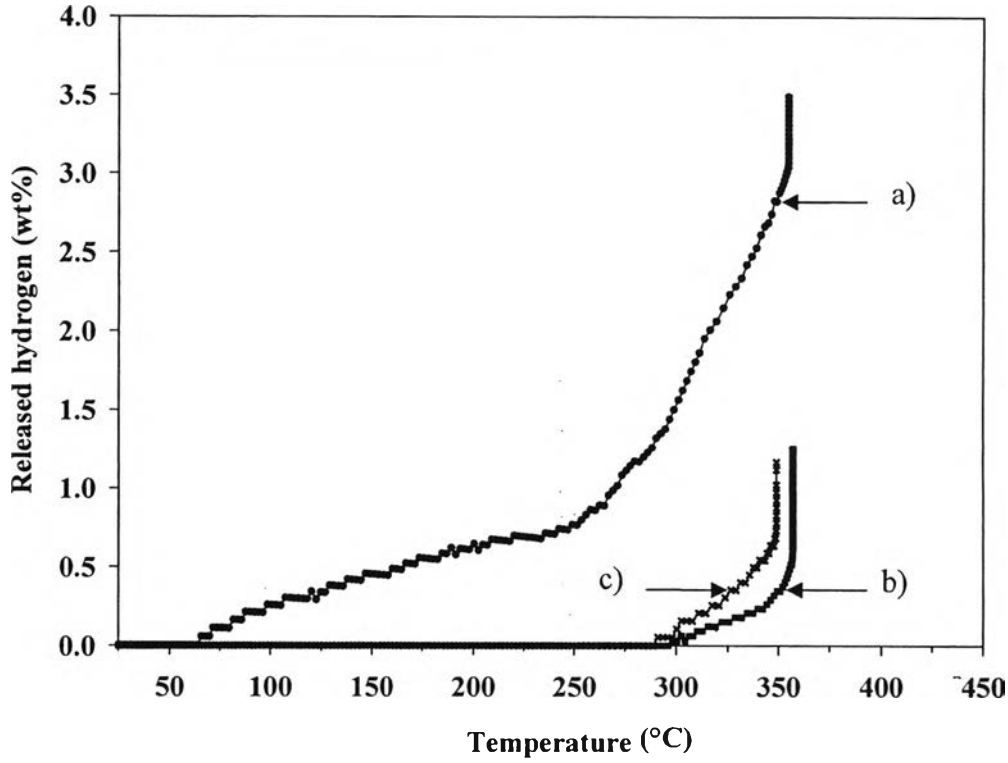

Figure 4.8 Correlation between temperature and hydrogen capacity during the desorption of 1 mol% $TiCl_3$–$LiBH_4$ in the: (a) 1st desorption; (b) 2nd desorption; and (c) 3rd desorption.

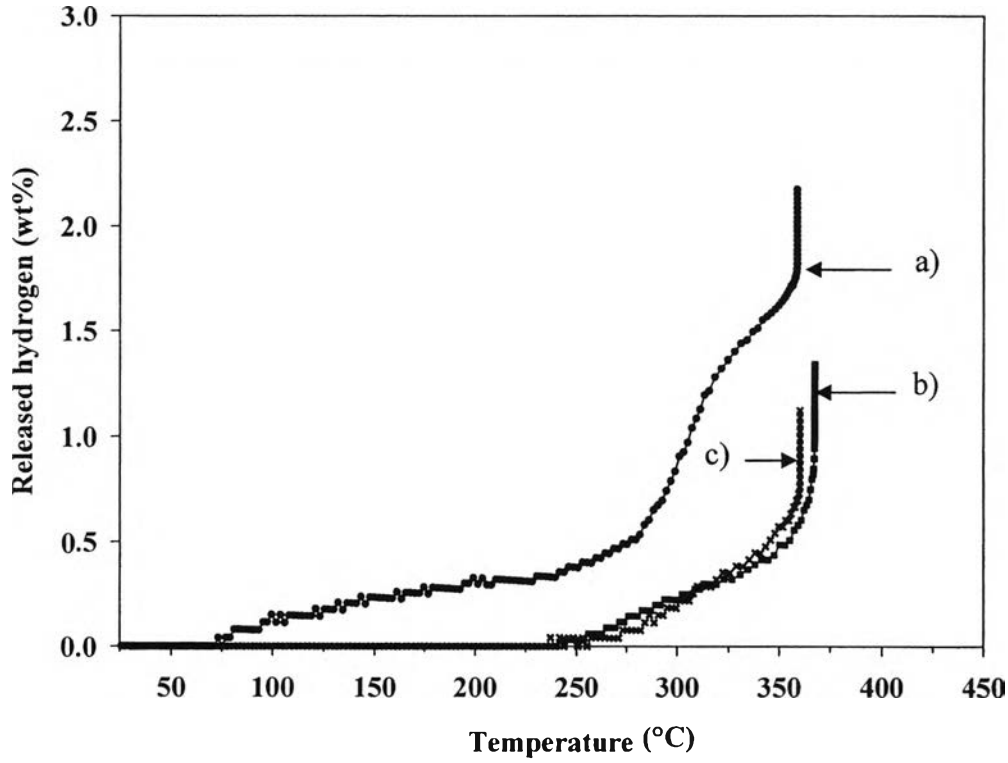

Figure 4.9 Correlation between temperature and hydrogen capacity during the desorption of 1 mol% TiO_2–$LiBH_4$ in the: (a) 1st desorption; (b) 2nd desorption; and (c) 3rd desorption.

4.4 Effect of Catalysts on Hydrogen Desorption in the Li–Al–B–H Systems

4.4.1 Effect of Catalysts

1 mol% of TiO_2, $TiCl_3$, VCl_3, or $ZrCl_4$ was added to the 2:1 $LiAlH_4$:$LiBH_4$ molar ratio mixture in order to investigate the effect of the transition metals on the hydrogen desorption/absorption behaviors. Figure 4.10 shows the two-step decomposition reactions and the decrease in the desorption temperature for all doped mixtures. The mixture in the presence of $TiCl_3$ starts to decompose and release hydrogen at the lowest temperature (40°C), which is lower than the undoped one by 60°C. In addition, 1 mol% $TiCl_3$–$2LiAlH_4$+$LiBH_4$ provides the highest amount of hydrogen desorption, 6.4 wt%, among the doped samples. However, the hydrogen desorption capacities of all the doped mixtures are significantly lower than that of the undoped one. The results were summarized in the Table 4.3.

4.4.2 Effect of $TiCl_3$ Loading

$TiCl_3$ at 3 and 5 mol% were further added to the $LiAlH_4$–$LiBH_4$ mixture. The results, as shown in Table 4.4 and Figure 4.11, exhibit that the hydrogen desorption capacities of all $TiCl_3$-doped mixtures are significantly lower than that of the undoped one. The hydrogen desorption capacity decreases with the increase in the doping amount, 6.4, 5.6, and 2.7 wt% for 1, 3, and 5 mol% doping, respectively. The desorption temperature of all $TiCl_3$-doped samples are lower than the undoped one by 40–70°C; however, there is no significant difference in the desorption temperature among the $TiCl_3$-doped samples.

Jin *et al.* (2008) reported that the mixture of $LiAlH_4$+2.2$LiBH_4$ together with 3 mol% TiF_3 started to decompose between 177°C and 247°C and the weight loss reached up to 7.2 wt% at 387°C. Mao *et al.* (2009) also reported that $LiAlH_4$+2$LiBH_4$ doped with 5 mol% TiF_3 could decrease the onset temperature of the first and second decomposition steps by 64 and 150°C, respectively. They further studied that doping with 5 mol% TiO_2 decreased the temperature of the first and second decomposition steps by 27 and 50°C, respectively.

4.4.3 Reversibility

In this work, no hydrogen absorption was observed for any of the doped samples at 300°C and under an 8.5 MPa hydrogen for 6 h.

Jin *et al.* (2008) confirmed that the dehydrogenated product of 3 mol% TiF_3–$LiAlH_4$+2.2$LiBH_4$ could be hydrogenated to about 5.1 wt% H_2 at 350°C and 70 bar hydrogen for 6 h. But the reaction kinetics was rather slow. Mao *et al.* (2009) reported that 5 mol% TiF_3–$LiAlH_4$+2$LiBH_4$ absorbed 3.76 wt% and 4.78 wt% in 1 h and 14 h, respectively, at 600°C and under 4 MPa hydrogen.

Table 4.3 Desorption amount (wt%) and temperature (°C) of doped $2LiAlH_4$+ $LiBH_4$ in the first (R1) and second (R2) steps

Sample	Desorption Temperature (°C)			Desorption Amount (wt%)		Total wt%
	R1	R2	Final	R1	R2	
$2LiAlH_4 + LiBH_4$	100	-	220	-	-	6.6
1 mol% TiO_2–	105	138	190	3.5	1.8	5.3
1 mol% $TiCl_3$–	40	110	170	4.4	2.0	6.4
1 mol% VCl_3–	53	110	155	3.7	1.8	5.5
1 mol% $ZrCl_4$–	72	105	150	4.3	1.8	6.1

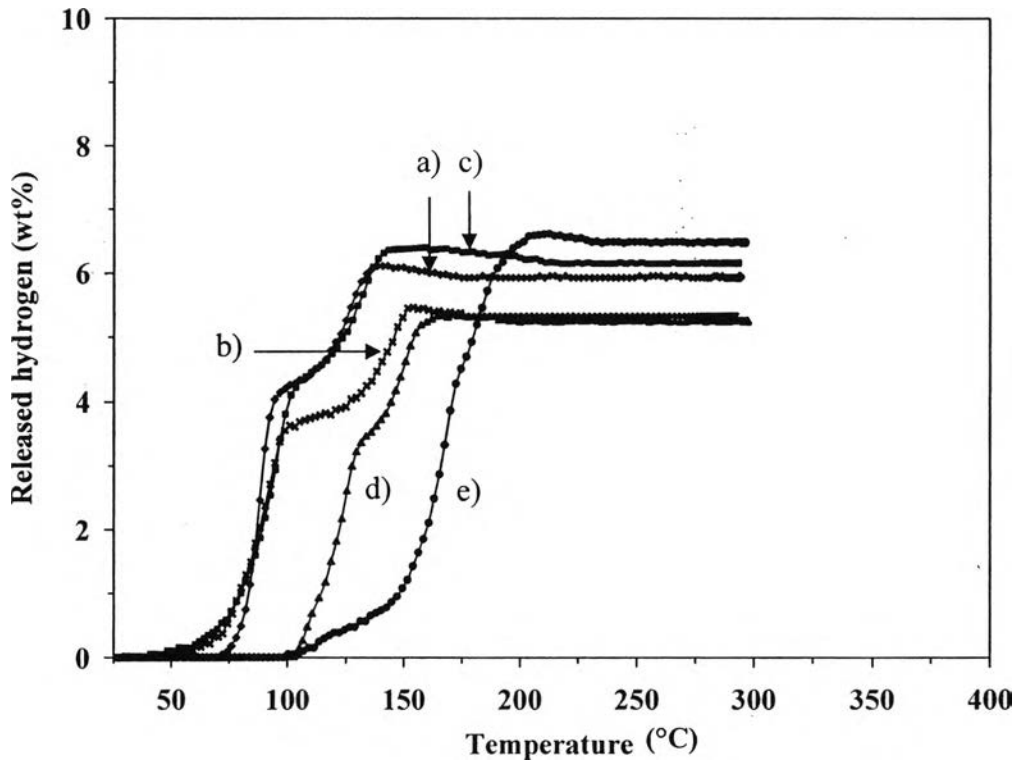

Figure 4.10 Correlation between temperature and hydrogen capacity during the desorption of: (a) 1 mol% $ZrCl_4$–$2LiAlH_4$+$LiBH_4$; (b) 1 mol% VCl_3–$2LiAlH_4$+$LiBH_4$; (c) 1 mol% $TiCl_3$–$2LiAlH_4$+$LiBH_4$; (d) 1 mol% TiO_2–$2LiAlH_4$+$LiBH_4$; and (e) $2LiAlH_4$+$LiBH_4$.

Table 4.4 Desorption amount (wt%) and temperature (°C) of $TiCl_3$-doped $2LiAlH_4$+ $LiBH_4$ in the first (R1) and second (R2) steps

Sample	Desorption Temperature (°C)			Desorption Amount (wt%)		Total wt%
	R1	R2	Final	R1	R2	
$2LiAlH_4 + LiBH_4$	100	-	220	-	-	6.6
1 mol% $TiCl_3$–	40	110	170	4.4	2.0	6.4
3 mol% $TiCl_3$–	60	95	170	3.1	2.5	5.6
5 mol% $TiCl_3$–	45	100	150	1.4	1.3	2.7

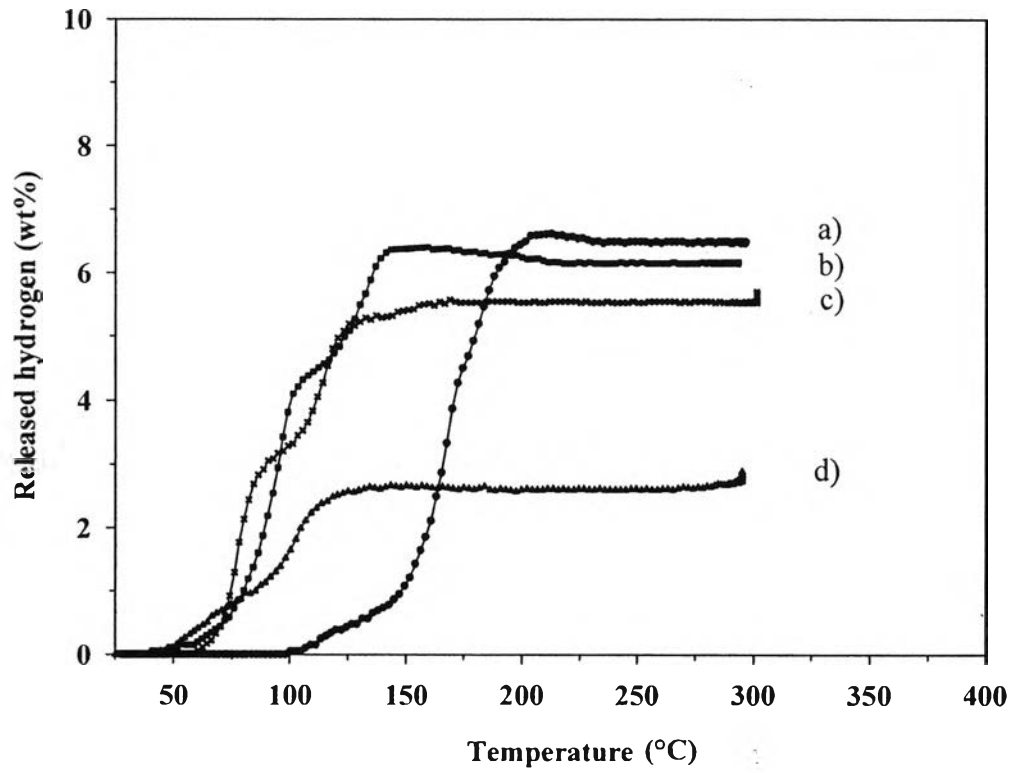

Figure 4.11 Correlation between temperature and hydrogen capacity during the desorption of: (a) $2LiAlH_4$+$LiBH_4$; (b) 1 mol% $TiCl_3$–$2LiAlH_4$+$LiBH_4$; (c) 3 mol% $TiCl_3$–$2LiAlH_4$+$LiBH_4$; and (d) 5 mol% $TiCl_3$–$2LiAlH_4$+$LiBH_4$.

4.5 Phase Transformation During the Desorption/Absorption

4.5.1 Phase Transformation During the Desorption/Absorption of Li–Al–H Systems

In this work, the X-ray diffraction (XRD) pattern of $LiAlH_4$ agree with Blanchard *et al.* (2004), who reported that $LiAlH_4$ decomposes into Li_3AlH_6, Al, and H_2 in the first step at 150–175°C as shown in reaction (4.1). Then, Li_3AlH_6 decomposes into LiH, Al, and H_2 in the second step at 180–220°C according to reaction (4.2). The total amount of the hydrogen desorption for the first and second steps is 7.9 wt%. And the last decomposition step occurs at a high temperature, about 400°C and releases 2.6 wt% hydrogen.

$$3LiAlH_4 \rightarrow Li_3AlH_6 + 2Al + 3H_2 \quad (4.1)$$

$$Li_3AlH_6 \rightarrow 3LiH + Al + \frac{3}{2}H_2 \quad (4.2)$$

$$3LiH + 3Al \rightarrow 3LiAl + \frac{3}{2}H_2 \quad (4.3)$$

The XRD pattern confirms that as-received $LiAlH_4$ composes of only $LiAlH_4$. In the case of undoped $LiAlH_4$, as shown in Figure 4.12, the XRD pattern indicates that only $LiAlH_4$ is left after the 15 min milling process. The hydrogen desorption was carried out from room temperature to 300°C. $LiAlH_4$ decomposes in the two-step reaction mechanism and releases 7.6 wt% of hydrogen between 145 and 220°C. After the hydrogen desorption, Al, LiH, and Li_3AlH_6 are identified in the dehydrogenated sample. Li_3AlH_6 decomposes incompletely in the second step, thus, Li_3AlH_6 is left in the sample after the hydrogen desorption.

In the case of doped $LiAlH_4$, as shown in Figures 4.13–4.16, all of the doped samples result in the same trend. Al is observed in the sample after the 120 min milling process. It is because of the partial decomposition of $LiAlH_4$ during the milling process. The milling and additive might destabilize the structure of $LiAlH_4$

(Suttisawat *et al.*, 2007). $LiAlH_4$ in the presence of a catalyst partially decomposes in the third step reaction (Eq. 4.3) because the total amounts of the hydrogen released for all doped samples are higher than 7.9 wt%. But no LiAl is observed for any of the doped samples. Only Al and LiH are left in the dehydrogenated sample after the hydrogen desorption at 300°C. The XRD technique cannot observe any peaks of the transition metal compound (Zr, V, or Ti) in the samples after the hydrogen desorption.

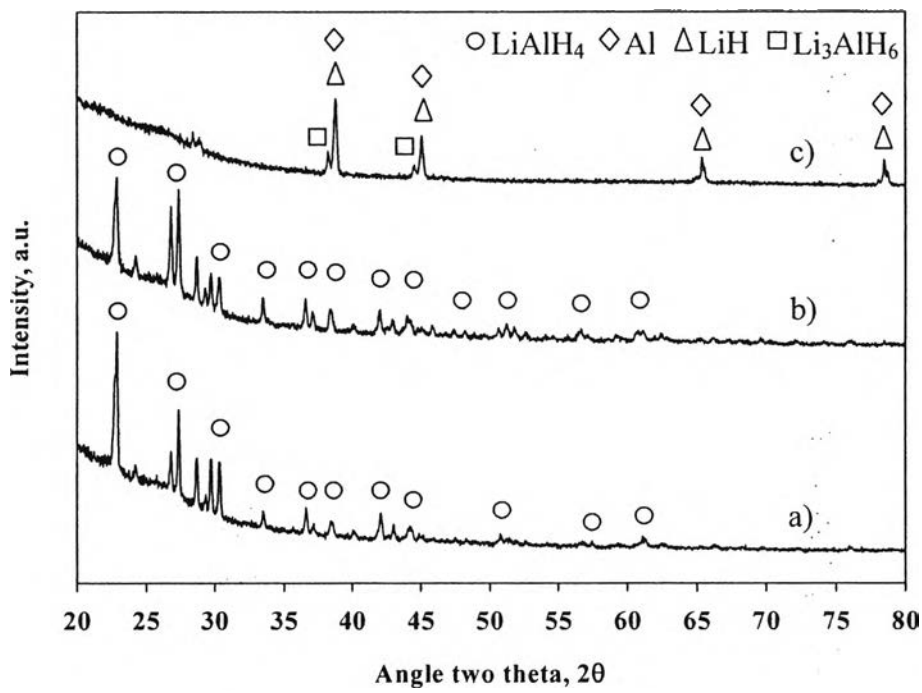

Figure 4.12 XRD patterns of: (a) as-received $LiAlH_4$; (b) milled $LiAlH_4$ for 15 min; and (c) desorbed $LiAlH_4$ at 300°C.

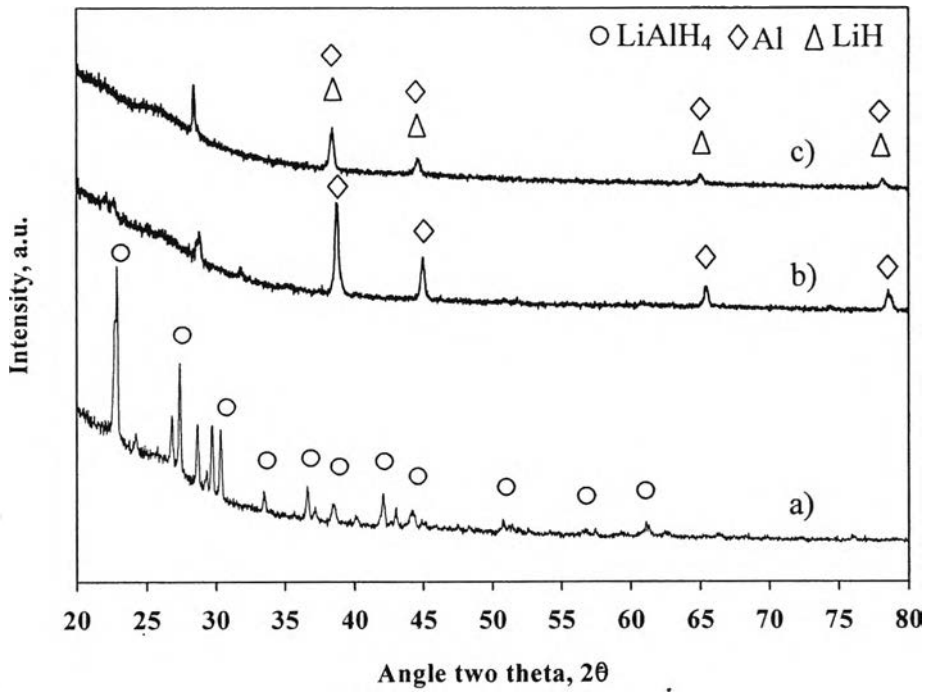

Figure 4.13 XRD patterns of: (a) as-received $LiAlH_4$; (b) milled 1 mol% $ZrCl_4$–$LiAlH_4$ for 120 min; and (c) desorbed 1 mol% $ZrCl_4$–$LiAlH_4$ at 300°C.

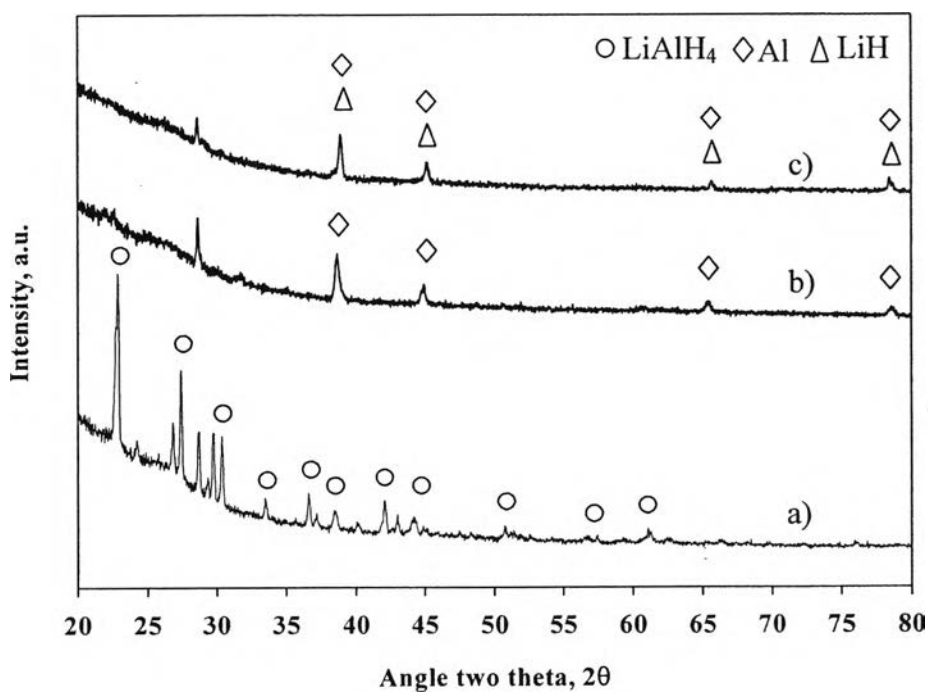

Figure 4.14 XRD patterns of: (a) as-received $LiAlH_4$; (b) milled 1 mol% VCl_3–$LiAlH_4$ for 120 min; and (c) desorbed 1 mol% VCl_3–$LiAlH_4$ at 300°C.

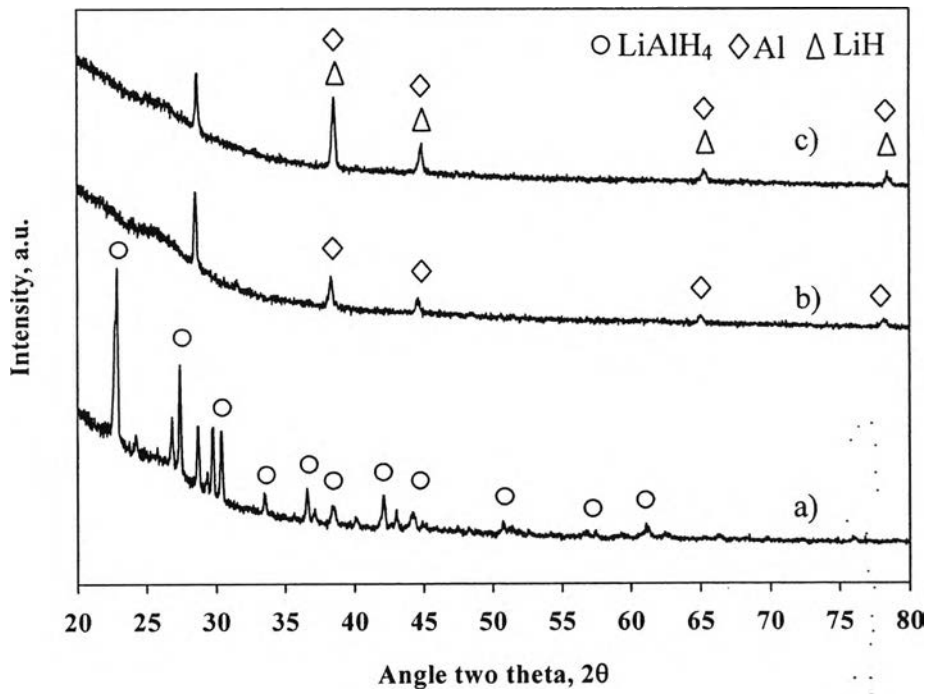

Figure 4.15 XRD patterns of: (a) as-received $LiAlH_4$; (b) milled 1 mol% $TiCl_3$–$LiAlH_4$ for 120 min; and (c) desorbed 1 mol% $TiCl_3$–$LiAlH_4$ at 300°C.

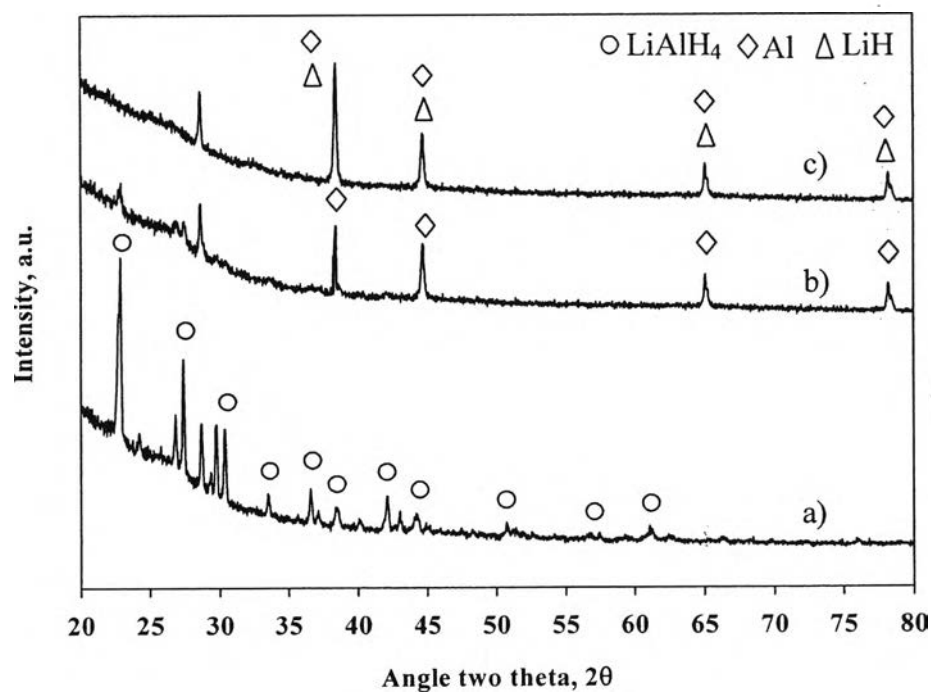

Figure 4.16 XRD patterns of: (a) as-received $LiAlH_4$; (b) milled 1 mol% TiO_2–$LiAlH_4$ for 120 min; and (c) desorbed 1 mol% TiO_2–$LiAlH_4$ at 300°C.

4.5.2 Phase Transformation During the Desorption/Absorption of Li–Al–B–H Systems

Phase transformation during the desorption of the 2:1 $LiAlH_4$:$LiBH_4$ molar ratio mixture is similar to the Li–Al–H systems. In the case of the undoped mixture, as shown in Figure 4.17, only $LiAlH_4$ is left after the 120 min milling process. The presence of Al and LiH is in the dehydrogenated sample after the hydrogen desorption at 300°C. In the case of the doped mixture, as shown in Figures 4.18–4.23, Al is observed after the milling process. As mentioned above, the milling process and a dopant might destabilize the structure of $LiAlH_4$. After the hydrogen desorption at 300°C, Al and LiH are left in the dehydrogenated samples. In addition, as shown in Figures 4.22–4.23, the XRD patterns of dehydrogenated samples in the presence of higher amount of the catalyst (3 or 5 mol% $TiCl_3$) exhibit the new peaks, which might be LiCl. And the formation of LiCl might deteriorate the hydrogen desorption ability of the samples. Then, it causes the decrease in the hydrogen desorption capacity.

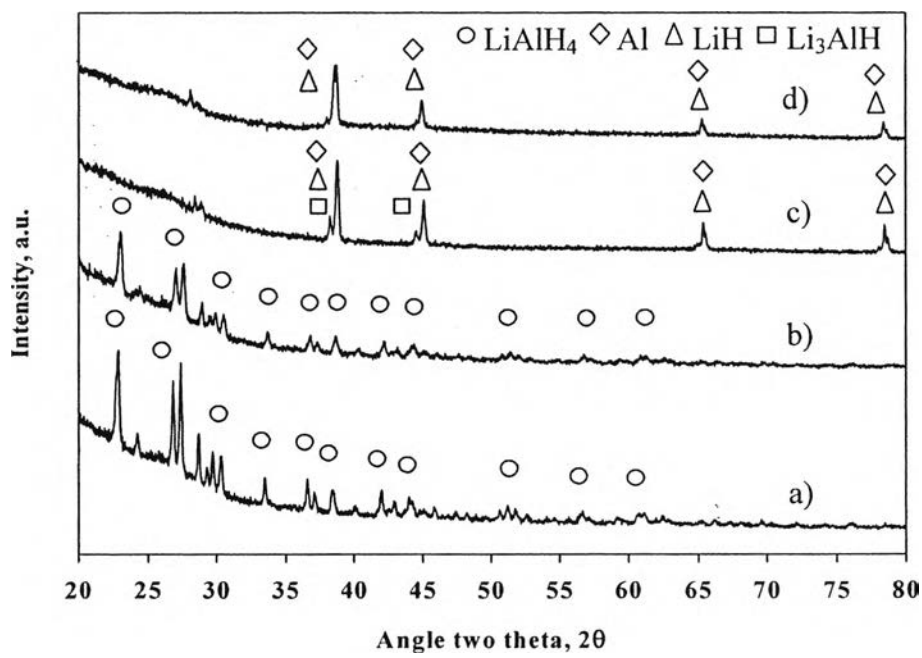

Figure 4.17 XRD patterns of: (a) milled $LiAlH_4$; (b) milled $2LiAlH_4$+$LiBH_4$ for 120 min; (c) desorbed $LiAlH_4$ at 300°C; and (d) desorbed $2LiAlH_4$+$LiBH_4$ at 300°C.

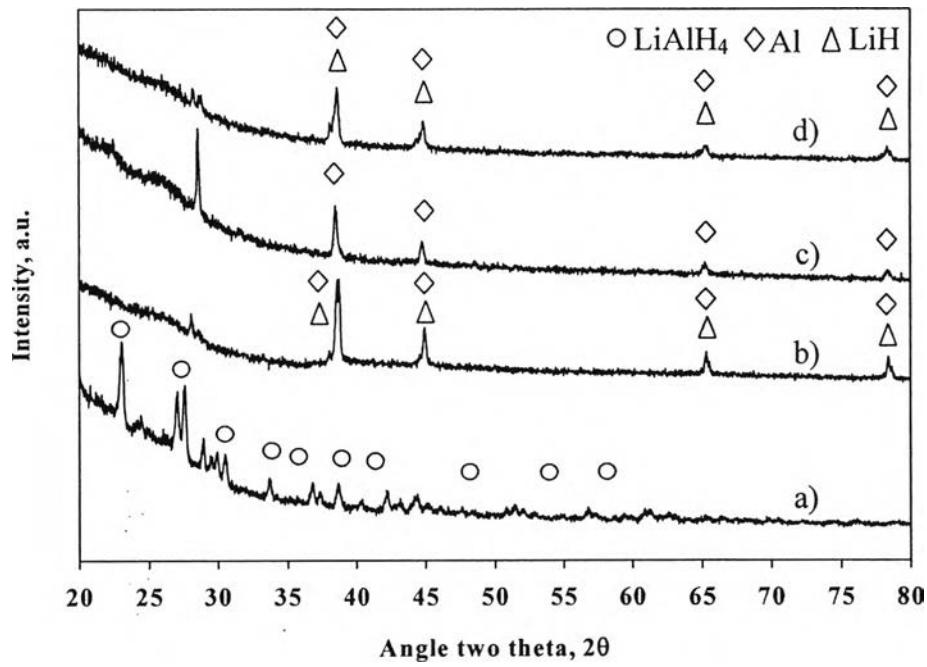

Figure 4.18 XRD patterns of : (a) milled $2LiAlH_4+LiBH_4$ for 120 min; (b) desorbed $2LiAlH_4+LiBH_4$ at 300°C; (c) milled 1 mol% $ZrCl_4$–$2LiAlH_4+LiBH_4$ for 120 min; and (d) desorbed 1 mol% $ZrCl_4$–$2LiAlH_4$+LiBH at 300°C.

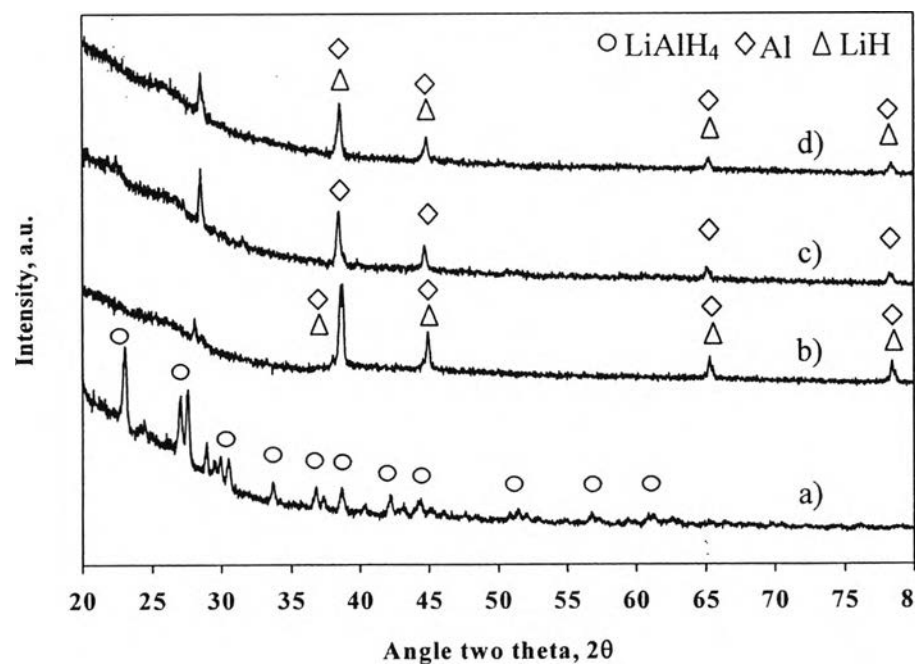

Figure 4.19 XRD patterns of : (a) milled $2LiAlH_4+LiBH_4$ for 120 min; (b) desorbed $2LiAlH_4+LiBH_4$ at 300°C; (c) milled 1 mol% VCl_3–$2LiAlH_4+LiBH_4$ for 120 min; and (d) desorbed 1 mol% VCl_3–$2LiAlH_4+LiBH_4$ at 300°C.

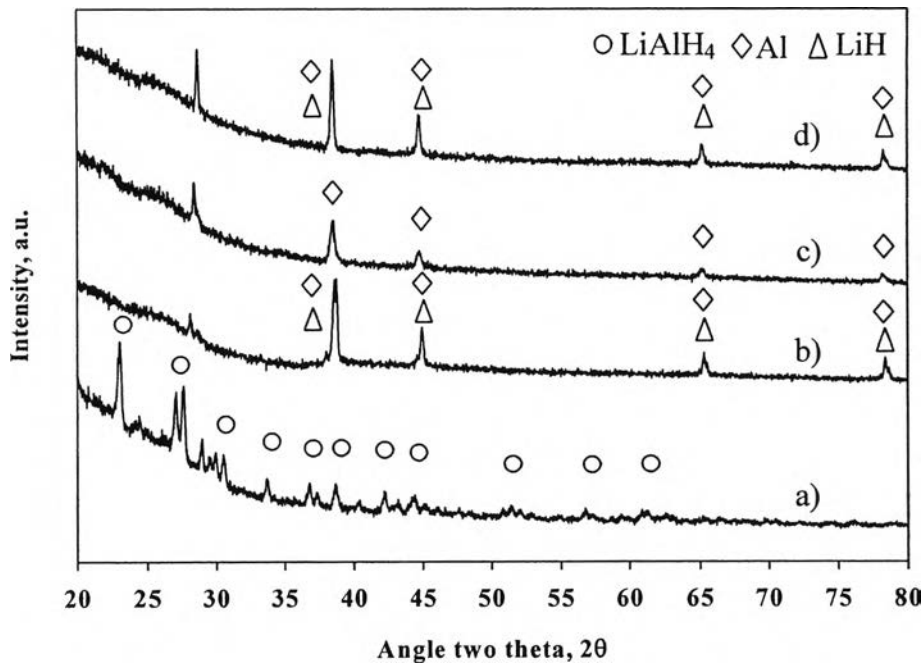

Figure 4.20 XRD patterns of : (a) milled $2LiAlH_4+LiBH_4$ for 120 min; (b) desorbed $2LiAlH_4+LiBH_4$ at 300°C; (c) milled 1 mol% TiO_2–$2LiAlH_4+LiBH_4$ for 120 min; and (d) desorbed 1 mol% TiO_2–$2LiAlH_4+LiBH_4$ at 300°C.

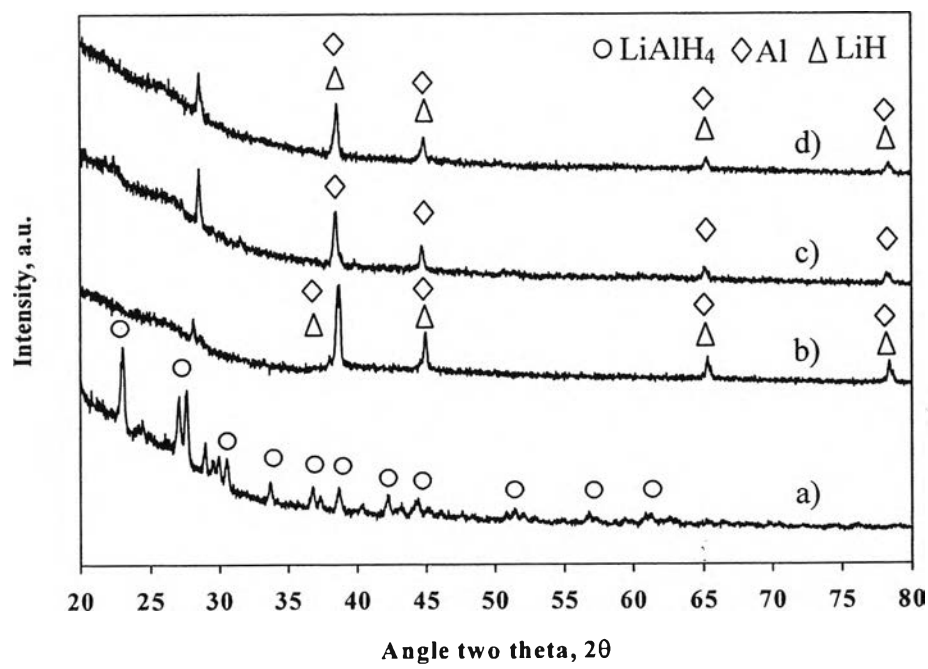

Figure 4.21 XRD patterns of : (a) milled $2LiAlH_4+LiBH_4$ for 120 min; (b) desorbed $2LiAlH_4+LiBH_4$ at 300°C; (c) milled 1 mol% $TiCl_3$–$2LiAlH_4+LiBH_4$ for 120 min; and (d) desorbed 1 mol% $TiCl_3$–$2LiAlH_4+LiBH_4$ at 300°C.

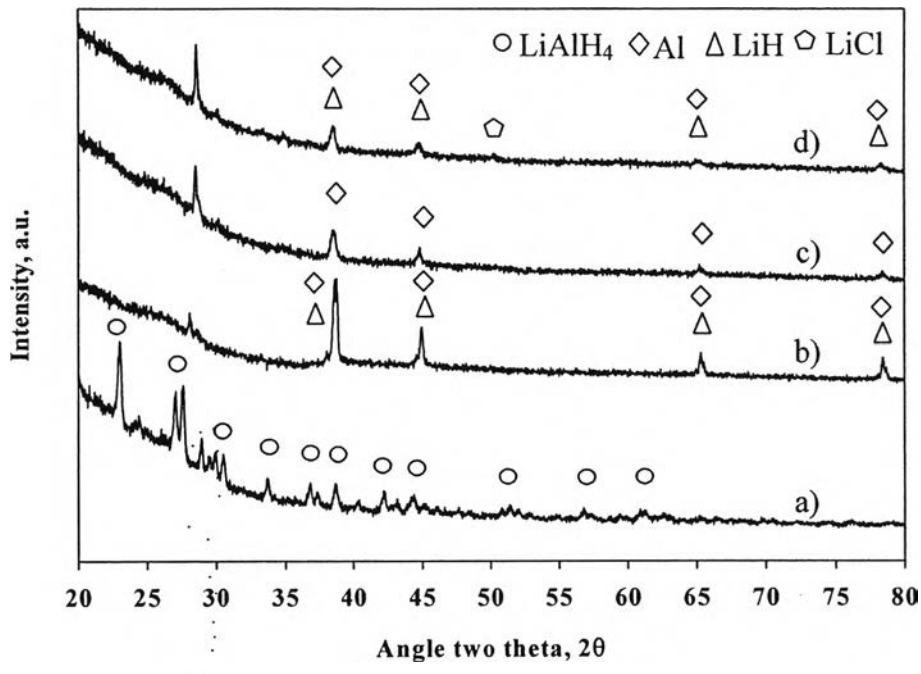

Figure 4.22 XRD patterns of : (a) milled $2LiAlH_4+LiBH_4$ for 120 min; (b) desorbed $2LiAlH_4+LiBH_4$ at 300°C; (c) milled 3 mol% $TiCl_3$–$2LiAlH_4+LiBH_4$ for 120 min; and (d) desorbed 3 mol% $TiCl_3$–$2LiAlH_4+LiBH_4$ at 300°C.

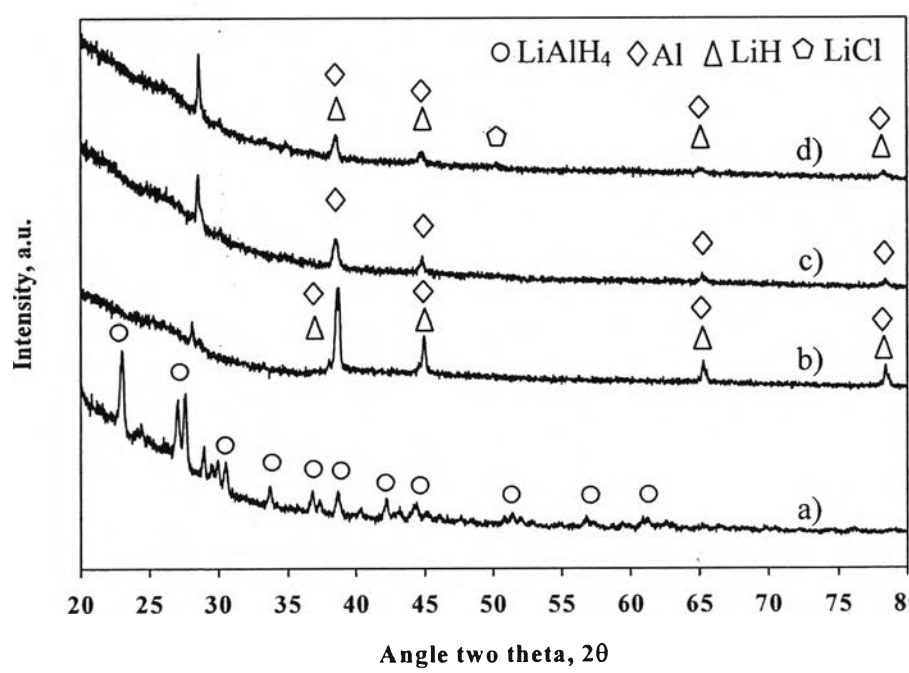

Figure 4.23 XRD patterns of : (a) milled $2LiAlH_4+LiBH_4$ for 120 min; (b) desorbed $2LiAlH_4+LiBH_4$ at 300°C; (c) milled 5 mol% $TiCl_3$–$2LiAlH_4+LiBH_4$ for 120 min; and (d) desorbed 5 mol% $TiCl_3$–$2LiAlH_4+LiBH_4$ at 300°C.

4.6 Roles of Metal Catalysts on the $LiAlH_4/LiBH_4$

$LiAlH_4$ and $LiAlH_4$–$LiBH_4$ mixture doped with TiO_2, $TiCl_3$, VCl_3, or $ZrCl_4$ partially decompose during the milling process because the structure of $LiAlH_4$ is unstable and the additives might destabilize the structure of $LiAlH_4$ (Suttisawat *et al.*, 2007). These metal catalysts in the hydride systems are reduced by the metal hydrides and transformed to TM-neutral (Blanchard *et al.*, 2004, Siangsai *et al.*, 2009), as shown in reactions (4.1) and (4.2), where TM is the transition metal, M is the metal, and X can be either V or Ti.

$$TiO_2 + 4MH \rightarrow 2M_2O + Ti + H_2 \tag{4.1}$$

$$XCl_3 + 3MH \rightarrow 3MCl + X + \frac{3}{2}H_2 \tag{4.2}$$

And it may be this reduction that increases the hydrogen desorption capacity of $LiAlH_4$ as compared to the undoped one. Moreover, after the decomposition, these catalysts can form M_2O and MCl, which are left in the sample as stable materials and cannot further decompose (Isobe *et al.*, 2005). In this work, MCl formation in the reaction (4.2) is LiCl since $LiAlH_4$ and $LiBH_4$ were investigated. The presence of LiCl might cause the decrease in the hydrogen capacity with the increase in the $TiCl_3$ amount.